Electronic Supplementary Material (ESI) for ChemComm.
This journal is © The Royal Society of Chemistry 2021

Supporting Information

Creating porosity in a trianglimine macrocycle by heterochiral pairing

Donglin He, Rob Clowes, Marc A. Little,* Ming Liu* and Andrew I. Cooper*

1. Experimental Details

1.1. Materials

(1*R*,2*R*)-1,2-Diaminocyclohexane was purchased from Manchester Organics, UK. Trifluoroacetic acid was purchased from Fisher Scientific, UK. All other chemicals and solvents (HPLC grade) were purchased from Sigma-Aldrich and used as received.

Table S1. Physical properties of *para*-xylene (*p*X), *meta*-xylene (*m*X), and *ortho*-xylene (*o*X)

Xylene isomer	Boiling point (°C)	Kinetic diameter (Å)	Molecular size (Å)[a]
*p*X	138.5	5.8	4.2*6.8
*m*X	139.1	6.4	4.8
*o*X	144.4	6.5	4.6

[a] The molecular size of the xylene isomers were calculated using the van der Waals Radii of the atoms.

1.2. Synthesis of Chiral 1

(1*R*,2*R*)-1,2-diaminocyclohexane or (1*S*,2*S*)-1,2-diaminocyclohexane (1.243 g, 10.89 mmol) was dissolved in acetonitrile (18 mL) and cooled to 0 °C. Isophthalaldehyde (1.460 g, 10.89 mmol) and a catalytic amount of trifluoroacetic acid (1 drop) were dissolved in acetonitrile (30 mL) and then added to the reaction. A white precipitate formed during the addition, and after being stirred at 0 °C for 30 minutes, the white precipitate was removed by filtration and washed three times with acetonitrile. Needle-shaped crystals of the pure product were isolated by recrystallising the crude product three times from ethyl acetate (EA) at 80 °C. Yield: 1.30 g (56.3%).

1.3. Synthesis of 1-*rac*

Equivalent molar amounts of **1**-*R* (50 mg, 0.079 mmol) and **1**-*S* (50 mg, 0.079 mmol) were dissolved in EA (50 mL) at 80 °C. The EA solution was then cooled down to room temperature and left to stand. Colourless block-shaped crystals of racemic **1**-*rac* were obtained after 1–2 days.

To generate the activated crystals of **1**-*rac*, the colourless block-shaped crystals were removed by filtration from EA. The crystals rapidly lost EA solvent in air to afford a polycrystalline white powder, which was then activated after heating at 80 °C under vacuum for 12 h. The single crystal of guest-free, **1**-*rac*, was obtained using this procedure.

1.4. Single Crystal Growth

Table S2. Methods of obtaining 1-*R* and 1-*rac* structures.

Crystal structures	Methods		
	Solution growth	Vapour diffusion	Desolvation
MeOH@**1**-*R*[a]	MeOH	n. r.	n. r.
1-*rac*[b]	EA	n. r.	Removal of EA at 80 °C
1*p*X@**1**-*rac*[c]	*p*X solution	*p*X or *p*X – *m*X mixture	n. r.
2*m*X@**1**-*rac*[d]	*m*X solution	n. r.	n. r.
3*o*X@**1**-*rac*[e]	*o*X solution	*o*X vapour	n. r.

[a] 5 mg dry **1**-*R* was dissolved in 2 mL of MeOH and then transferred into small glass sample vials by filtration. The resultant homogenous solution was allowed to slowly evaporate at room temperature over 3 to 5 days to afford colourless crystals.
[b] Experimental details are included in Section 1.3.
[c]-[e] 5 mg dry **1**-*rac* was dissolved in 2 mL of *p*X, *m*X, *o*X and then transferred into small glass sample vials by filtration. The resultant homogenous solutions were then allowed to slowly evaporate at room temperature over 5 to 12 days to afford colourless crystals.

1.5. Methods

1.5.1 Solution NMR: Solution ^{1}H NMR spectra were recorded at 400.13 MHz using a Bruker Avance 400 NMR spectrometer.

1.5.2 Thermogravimetric analysis: TGA analysis was carried out using a Q5000IR analyzer (TA instruments) with an automated vertical overhead thermobalance. The samples were heated at the rate of 10 °C /min using dry N_2 as the protective gas.

1.5.3 Powder X-ray Diffraction (PXRD): For screening, PXRD patterns were collected in transmission mode on samples held on thin Mylar film in aluminum well plates on a Panalytical Empyrean diffractometer, equipped with a high throughput screening XYZ stage, X-ray focusing mirror, and PIXcel detector, using Cu-Kα (λ = 1.541 Å) radiation. For indexing, samples were loaded into borosilicate glass capillaries, and PXRD patterns were recorded in transmission mode on a Panalytical Empyrean diffractometer, equipped with a sample spinner, X-ray focusing mirror, and PIXcel detector, using Cu-Kα (λ = 1.541 Å) radiation. PXRD patterns were refined with Pawley refinement in TOPAS Academic.

1.5.4 Single crystal X-ray diffraction (SC-XRD): SC-XRD data sets were measured on a Rigaku MicroMax-007 HF rotating anode diffractometer (Mo-Kα radiation, λ = 0.71073 Å, Kappa 4-circle goniometer, Rigaku Saturn724+ detector); or at beamline I19, Diamond Light Source, Didcot, UK using silicon double crystal monochromated synchrotron radiation (λ = 0.6889 Å, Pilatus 2M detector). Absorption corrections, using the multi-scan method, were performed with the program CrysAlisPro 1.171.40.45a. For synchrotron X-ray data, collected at Diamond Light Source, data reduction and absorption corrections were performed with xia2.[1] Structures were solved with SHELXT,[2] and refined by full-matrix least-squares on $|F|^2$ by SHELXL,[3] interfaced through the program OLEX2.[4] H atom positions for the C-H groups were refined using the riding model. For full refinement details, see supporting CIF files. Supplementary CIF files for MeOH@**1**-*R* (CCDC Reference: 2073635), EA@**1**-*rac* (2073632) **1**-*rac* (2073633), 1*p*X@**1**-*rac* (2073634), 3*m*X@2(**1**-*rac*) (2073637), 2*o*X@**1**-*rac* (2073636), which include structure factors, have been deposited in the CCDC.

1.5.5 Gas sorption: Nitrogen adsorption and desorption isotherms for all samples were collected at 77 K using an ASAP2020 volumetric adsorption analyzer (Micrometrics Instrument Corporation). Carbon dioxide and hydrogen isotherms were collected up to a pressure of 1200 mbar on a Micromeritics ASAP2020 at 77 K for hydrogen, or at 273 and 298 K for carbon dioxide. All samples were degassed at 80 °C for 15 hours under a dynamic vacuum (10−5 bar) before analysis.

2. Crystallography Report

Table S2. SC-XRD data for MeOH@**1**-*R* and activated **1**-*rac*.

Molecule	MeOH@**1**-*R*[a]	EA@**1**-*rac*[b]	**1**-*rac*
Crystallisation Solvent	methanol	EA	EA
Space Group	$P6_3$	$P\bar{1}$	$I2/a$
Wavelength [Å]	Mo-Kα	Mo-Kα	Mo-Kα
Collection Temperature	100 K	100 K	100 K
Formula	$C_{42}H_{48}N_6$, $0.75(C_6H_{24}O_6)$	$2(C_{42}H_{48}N_6)$, $2(C_4H_8O_2)$, $2(H_2O)$	$C_{42}H_{48}N_6$
Mr	660.89	1481.93	636.86
Crystal Size (mm)	0.36×0.25×0.14	0.25×0.19×0.16	0.30×0.21×0.11
Crystal System	hexagonal	triclinic	monoclinic
a [Å]	20.450(2)	14.3324(6)	24.7909(8)
b [Å]	= *a*	14.3555(6)	14.7339(4)
c [Å]	5.9423(5)	25.1851(9)	22.7185(8)
α [°]	90	89.815(3)	90
β [°]	90	77.839(4)	101.230(3)
γ [°]	120	60.849(4)	90
V [Å^3]	2152.2(5)	4393.8(3)	8139.4(5)
Z	2	2	8
D_{calcd} [g cm^{-3}]	1.020	1.120	1.039
μ [mm^{-1}]	0.062	0.071	0.062
F(000)	711	1592	2736
2θ range [°]	6.08 – 43.88	3.27 – 52.85	3.22 – 52.74
Reflections collected	19869		52053
Independent reflections, R_{int}	1724, 0.1107	27498	8312, 0.0594
Obs. Data [$I > 2\sigma$]	1504	16482	5734
Data / restraints / parameters	1724/3/154	27498 / 30 / 994	8312/0/433
Final R_1 values ($I > 2\sigma(I)$)	6.46%	8.21%	6.28%
Final R_1 values (all data)	7.57%	12.41%	10.02%
Final $wR(F^2)$ values (all data)	16.37%	22.77%	15.03%
Goodness-of-fit on F^2	1.078	1.203	1.042
Largest difference peak and hole [e.A^{-3}]	0.397/-0.173	0.710/-0.357	0.213/-0.196
CCDC	2073635	2073632	2073633

[a] Residual electron density in the crystal structure that was within 3 Å of N6 was tentatively modelled as partially H_2O without riding H atoms. However, this electron density could indicate unresolved *m*X disorder. [b] the structure refined as a 2-component twin with HKLF5 reflection file and BASF refined to 0.4661(12). Attempts were made to resolve all the disordered EA solvent molecules in the **1** cavities, but some residual electron density was modelled as disordered O atoms.

Table S3. SC-XRD data for xylene loaded **1**-*rac* structures.

Molecule	1*p*X@**1**-*rac*	3*m*X@2(**1**-*rac*)	2*o*X@**1**-*rac*
Crystallisation Solvent	*p*X	*m*X	*o*X
Space Group	*C*2/*c*	$P2_1/c$	$P\bar{1}$
Wavelength [Å]	Mo-Kα	Mo-Kα	0.6889
Collection Temperature	100 K	100 K	100 K
Formula	$C_{42}H_{48}N_6$, 2(0.5(C_8 H_{10})	2($C_{42}H_{48}N_6$), 3(C_8H_{10})	$C_{42}H_{48}N_6$, 2(C_8H_{10})
Mr	743.02	1594.0	849.18
Crystal Size (mm)	0.54×0.28×0.09	0.45×0.19×0.10	0.1×0.06×0.02
Crystal System	monoclinic	monoclinic	triclinic
a [Å]	25.2103(4)	29.9687(5)	11.19190(7)
b [Å]	14.0669(2)	22.3149(3)	15.18470(8)
c [Å]	25.3934(4)	14.6297(2)	15.73550(8)
α [°]	90	90	104.5050(4)
β [°]	102.506(2)	103.221(2)	91.5770(5)
γ [°]	90	90	105.6390(5)
V [Å^3]	8791.6(2)	9524.3(3)	2480.11(2)
Z	8	4	2
D_{calcd} [g cm^{-3}]	1.123	1.112	1.137
μ [mm^{-1}]	0.066	0.065	0.062
F(000)	3200	3436	916.0
2θ range [°]	3.56 – 66.15	3.65 – 52.78	2.60 – 51.69
Reflections collected	70247	133758	32622
Independent reflections, R_{int}	15555, 0.0536	19494, 0.0762	10349, 0.1264
Obs. Data [$I > 2\sigma$]	11060	13778	9404
Data / restraints / parameters	15555/0/507	19494/160/1147	10349/112/632
Final R_1 values ($I > 2\sigma(I)$)	6.37%	6.68%	6.74%
Final R_1 values (all data)	9.63%	9.99%	7.41%
Final $wR(F^2)$ values (all data)	15.59%	14.81%	19.55%
Goodness-of-fit on F^2	1.015	1.065	1.077
Largest difference peak and hole [e.A^{-3}]	0.336/-0.369	0.387 / -0.198	0.521/-0.398
CCDC	2073634	2073637	2073636

3. Characterization

3.1 NMR Spectra

The **1**-*R* and **1**-*rac* samples were recrystallized from EA. The resultant crystals were isolated by filtration from EA and then dried under a dynamic vacuum at 80 °C. After activation, the crystals were characterized by ^{1}H NMR, and the spectra of activated **1**-*R* and **1**-*rac* in CD_2Cl_2 are shown in Figure S1-S2: ^{1}H NMR (CD_2Cl_2) δ 1.46-1.72 (m, 24H, cyclohexyl CH_2 and CH groups), 3.33-3.40 (m, 6H, CHN), 7.24 (t, 3H, ArH), 7.56 (broad s, 6H, ArH), 7.89 (s, 3H, ArH), 8.15 (s, 6H, CH=N). The ^{1}H NMR spectrum of **1** is consistent with literature reported data.[5]

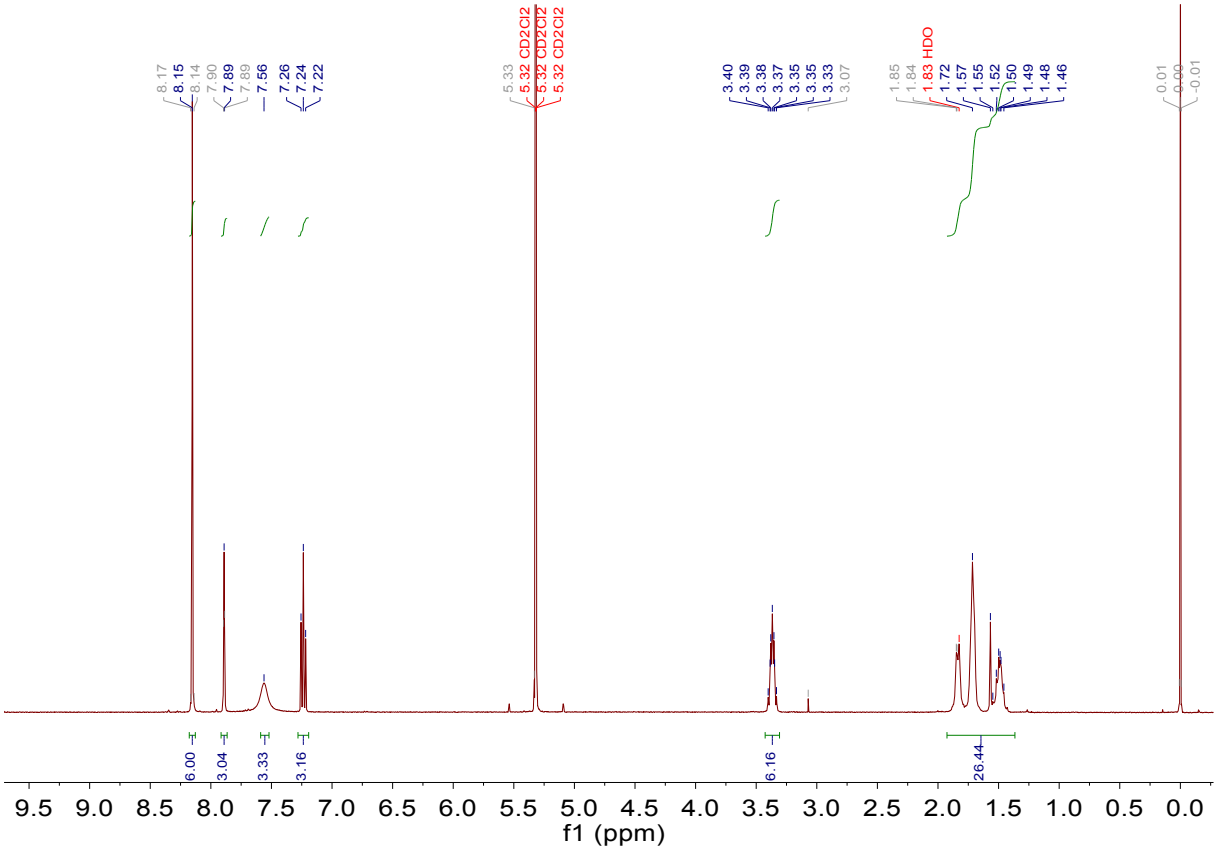

Figure S1. ^{1}H NMR spectrum (400 MHz, CD_2Cl_2, 293 K) of **1**-*R* after activation at 80 °C.

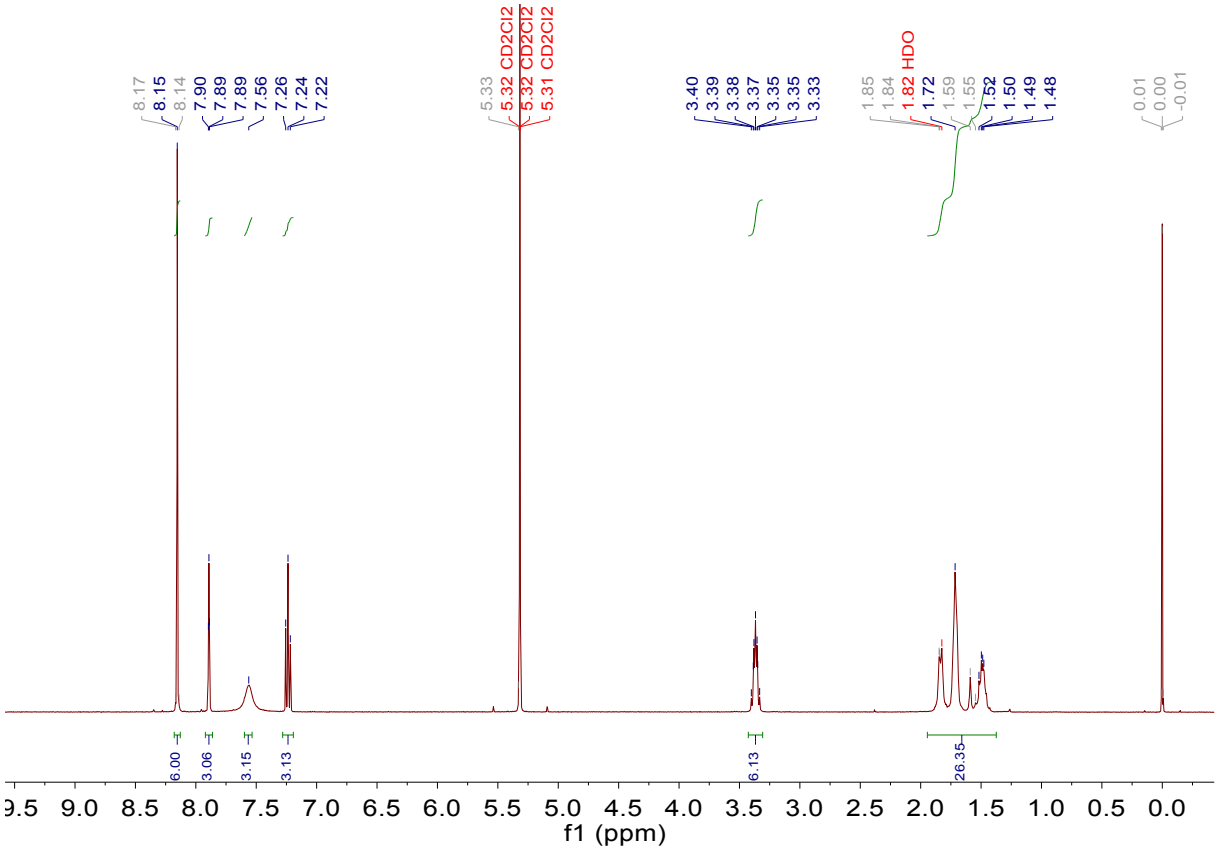

Figure S2. ^{1}H NMR spectrum (400 MHz, CD_2Cl_2, 293 K) of **1**-*rac* after activation at 80 °C.

Procedure used for **1**-*rac* vapour adsorption experiments: An open 5 mL vial containing 3.5 mg of guest-free **1**-*rac* adsorbent was placed in a sealed 20 mL vial containing 0.5 mL pure *p*X, pure *m*X, pure *o*X, and 1:1 (*vol*:*vol*) or 1:1:1 (*vol*:*vol*:*vol*) mixtures of *p*X, *m*X, and *o*X. The resultant crystals were dried at room temperature for 30-45 min. Afterward, the crystals were characterized by ^{1}H NMR after fully dissolving the sample in CD_2Cl_2.

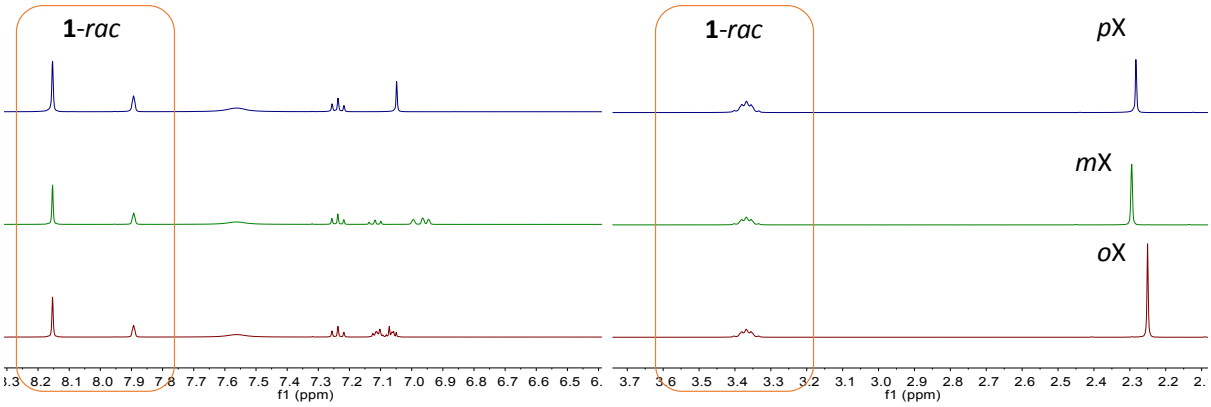

Figure S3. ^{1}H NMR spectrum (400 MHz, CD_2Cl_2) of **1**-*rac* after vapour adsorption of *p*X, *m*X, or *o*X for 5.5 h.

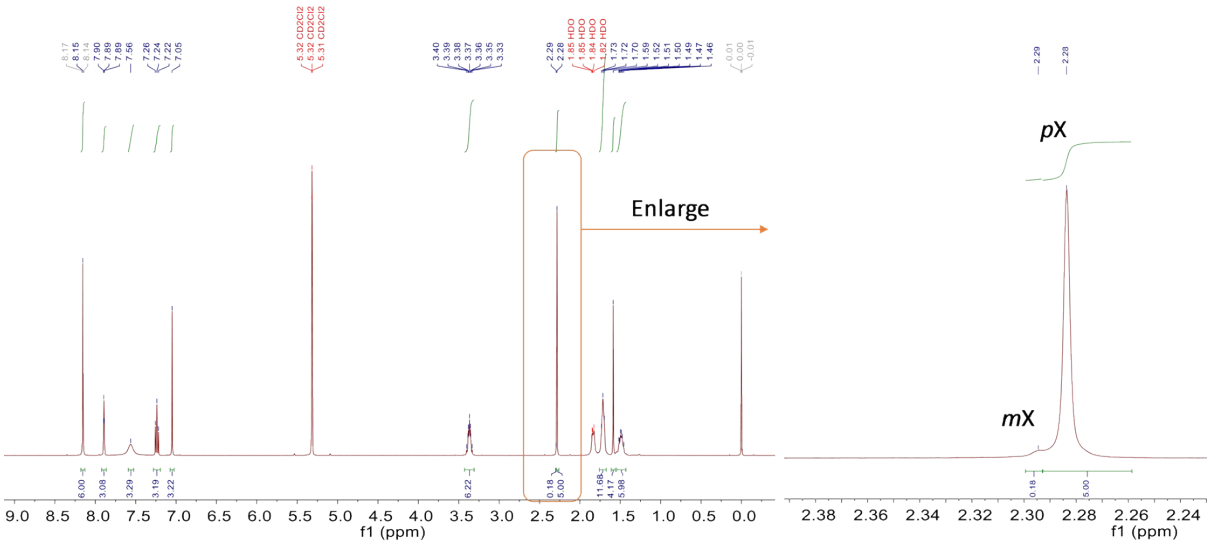

Figure S4. ^{1}H NMR spectrum (400 MHz, CD_2Cl_2) of **1**-*rac* after vapour adsorption of the *p*X:*m*X (1:1, *vol*:*vol*) mixture for 10 h. The relative uptake of *p*X and *m*X adsorbed by **1**-*rac* is plotted in Figure 4b.

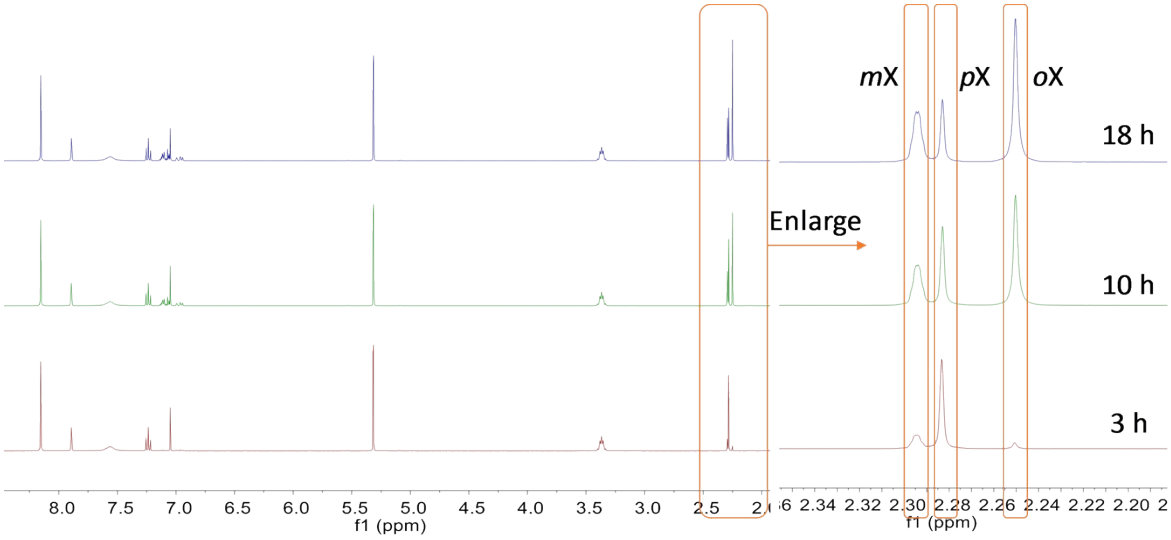

Figure S5 ^{1}H NMR spectra (400 MHz, CD_2Cl_2) from time-dependent vapour adsorption experiments for **1**-*rac* after exposure to the *p*X:*m*X:*o*X (1:1:1, *vol*:*vol*:*vol*) mixture. From bottom to top, the spectra were recorded at 3h, 10 h, and 18 h. The relative uptakes of *p*X, *m*X, and *o*X adsorbed by **1**-*rac* during this experiment are plotted in Figure S16.

3.2 TGA data

An open 5 mL vial containing 3.5 mg of guest-free **1**-*rac* adsorbent was placed in a sealed 20 mL vial containing 0.5 mL pure *p*X or pure *m*X or pure *o*X for 14 h. Afterward, the crystals were characterized by TGA with N_2 gas flow.

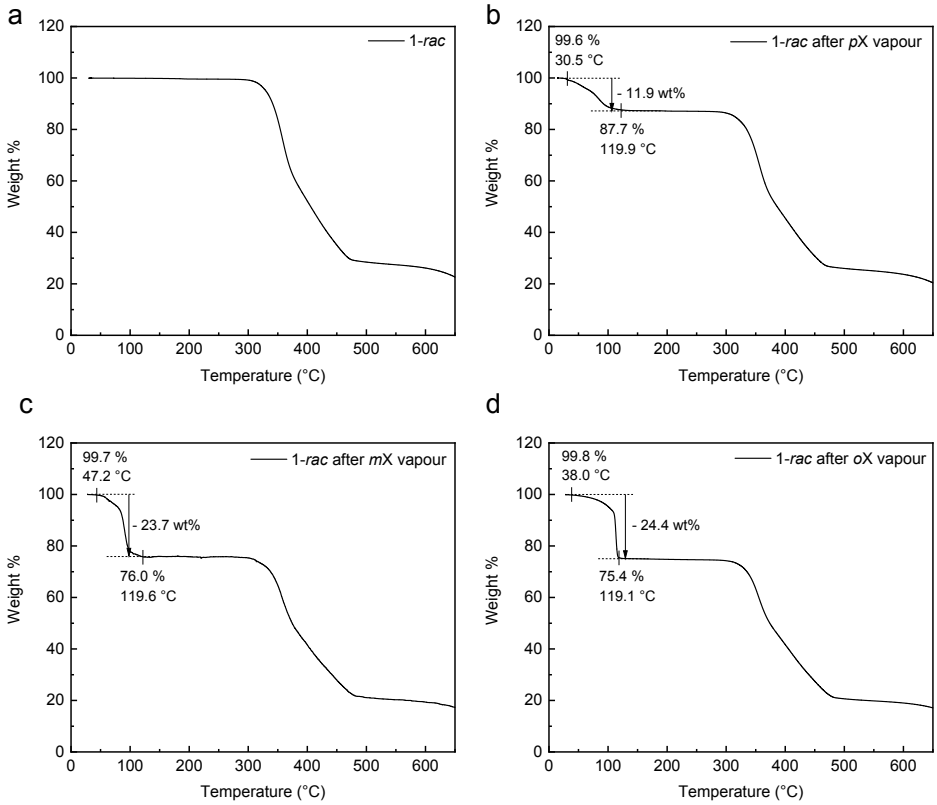

Figure S6. Thermogravimetric analysis of a) **1**-*rac*. b) **1**-rac after adsorption of *p*X. c) **1**-rac after adsorption of *m*X. c) **1**-rac after adsorption of *o*X. To generate the xylene loaded materials, **1**-rac was exposed to vapours of the pure xylene isomers for 14 hours at room temperature in a sealed vial.

3.3 PXRD Data

1-*rac* after vapour adsorption: an open 5 mL vial containing 3.5 mg of guest-free **1**-*rac* adsorbent was placed in a sealed 20 mL vial containing 0.5 mL of pure *p*X, pure *m*X, pure *o*X, and 1:1 (*vol*:*vol*) or 1:1:1 (*vol*:*vol*:*vol*) mixtures of *p*X, *m*X, and *o*X. The resultant crystals were evaporated at room temperature for 30-45 min. Afterward, the solids were characterized by PXRD.

Activation of **1**-*rac* after vapour adsorption: an open 5 mL vial containing 3.5 mg of guest-free **1**-*rac* adsorbent was placed in a sealed 20 mL vial containing 0.5 mL of pure *p*X, pure *m*X, pure *o*X, and 1:1 (*vol*:*vol*) or 1:1:1 (*vol*:*vol*:*vol*) mixtures of *p*X, *m*X, and *o*X. Initially, the resultant crystals were evaporated at room temperature for 30-45 min. Afterward, the solids dried under vacuum at either 80, 100, 120, or 140 °C, before PXRD patterns were recorded after cooling the solids to room temperature.

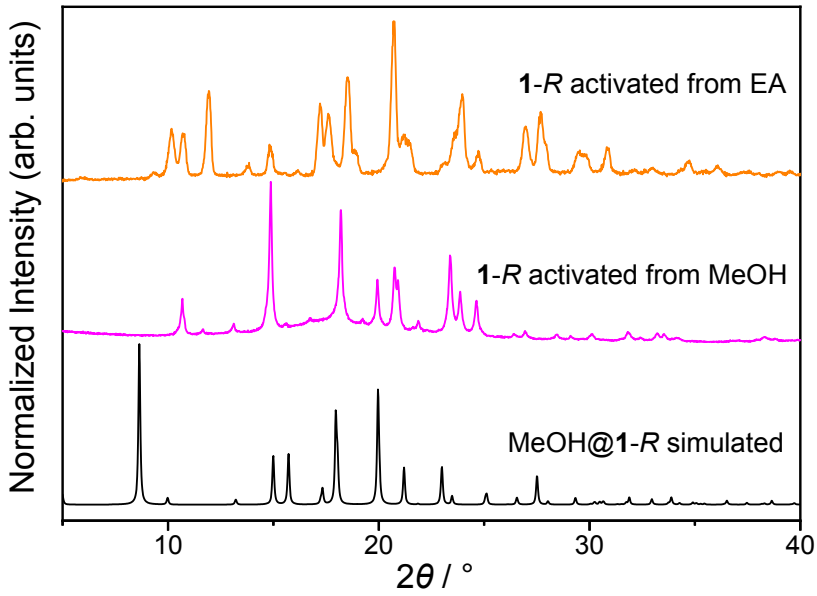

Figure S7. PXRD patterns of activated **1**-*R* recrystallized from EA and dried at 80 °C under vacuum (top), activated **1**-*R* recrystallized from MeOH and dried at 80 °C under vacuum (middle), and simulated PXRD pattern of solvated **1**-*R* recrystallized from MeOH (bottom).

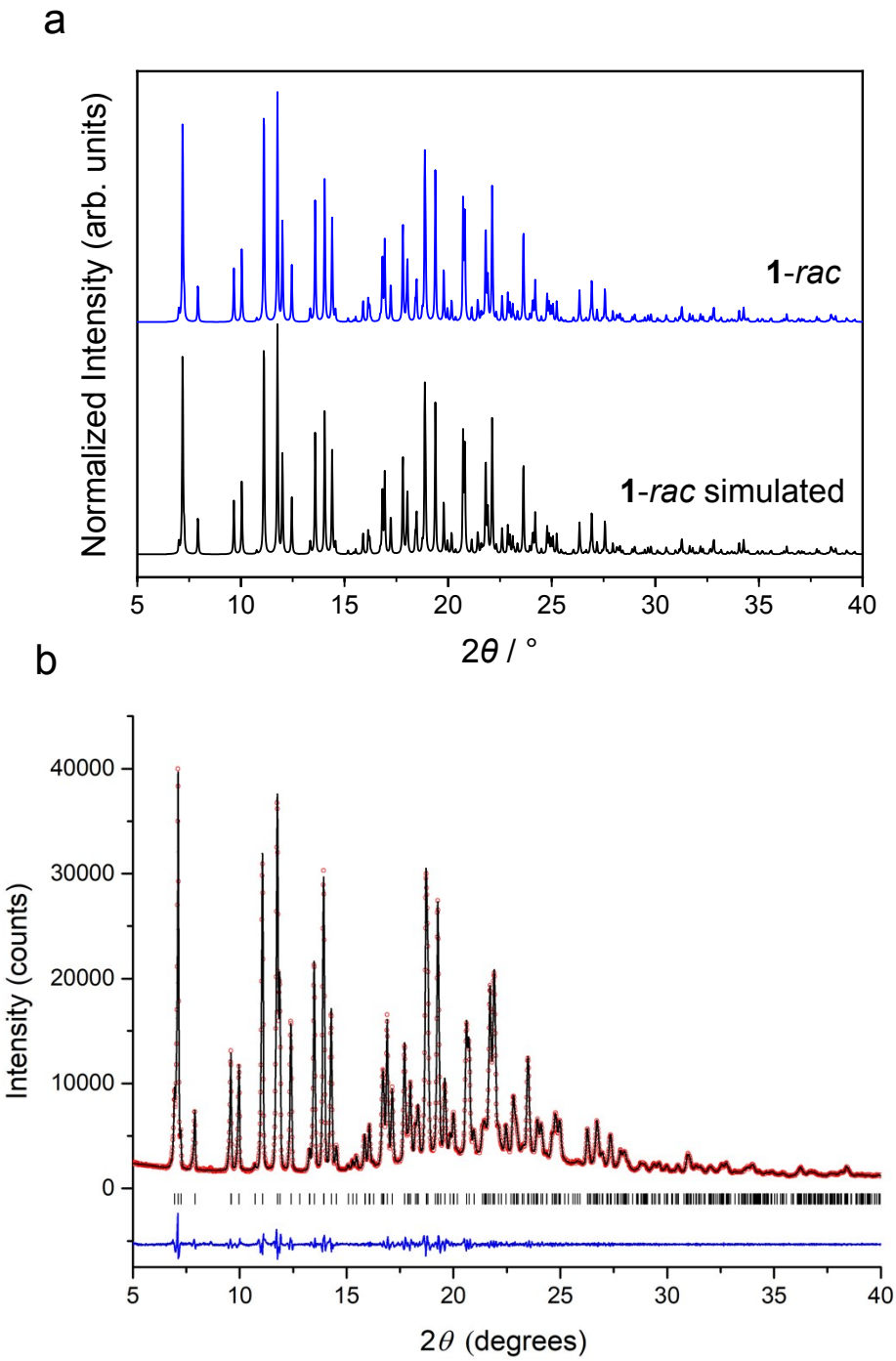

Figure S8. (a) PXRD patterns of activated **1**-*rac* recrystallized from EA and dried at 80 °C under vacuum (top), and simulated PXRD pattern of activated **1**-*rac* (bottom). (b) Pawley refinement of **1**-*rac* that was refined using the monoclinic *I* centred symmetry used to refine the single crystal structure. Final observed (red), calculated (black) and difference (blue) PXRD profiles for Pawley refinement (R_{wp} = 3.26%, R_p = 2.38%, χ^2 = 2.20, *a* = 24.8713(5) Å, b = 14.8879(3) Å, *c* = 22.8102(5) Å; β = 101.577(2)°; *V* = 8274.4(3) Å^3, *I*2/*a*).

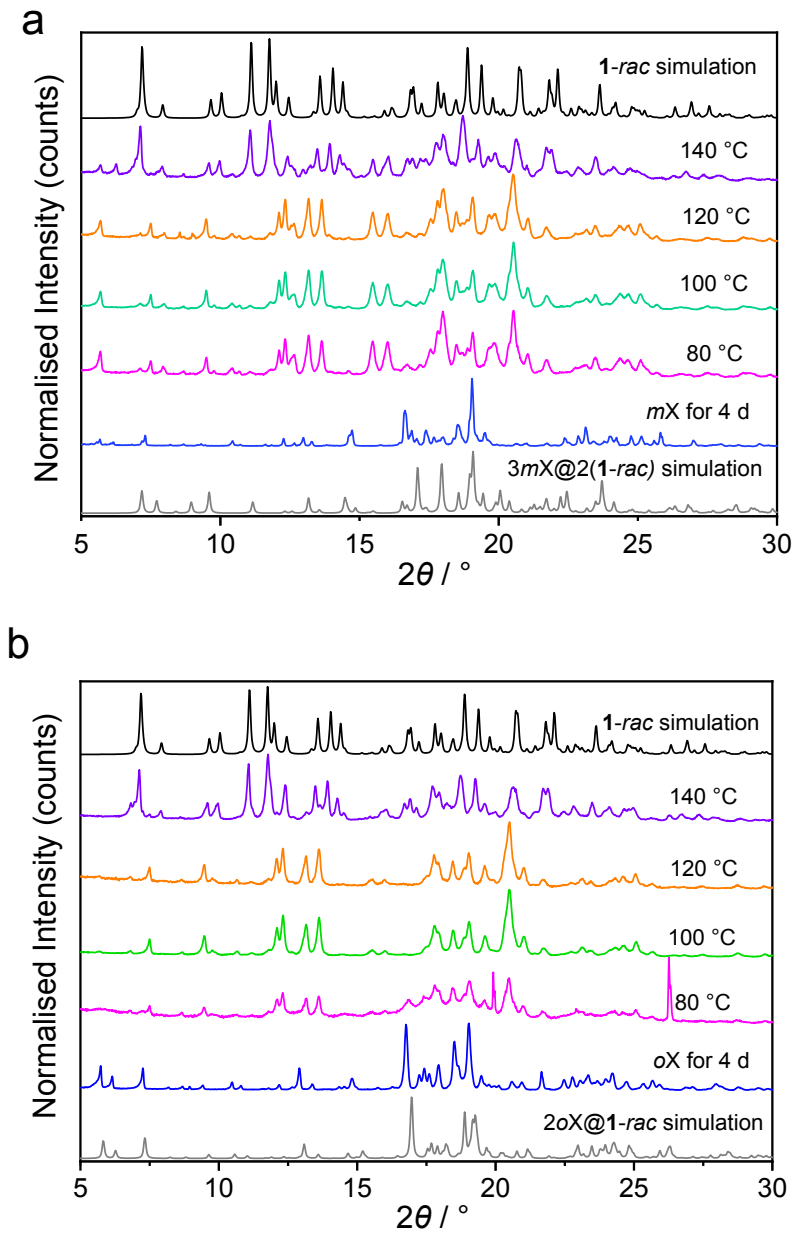

Figure S9. (a) PXRD patterns for samples of **1**-*rac* after being exposed to *m*X vapour and then dried under vacuum at elevated temperatures. We observed the phase of **1**-*rac* adsorbed the *m*X gradually transforming back to **1**-*rac* when being dried under vacuum. The sample had completely transformed to **1**-*rac* after thermal activation at 140 °C. (b) PXRD patterns for samples of **1**-*rac* after being exposed to *o*X vapour and then dried under vacuum at elevated temperatures. We observed 2*o*X@**1**-*rac* gradually transform back to **1**-*rac* after being activated under vacuum at higher temperatures, with the sample completely transforming back to **1**-*rac* after thermal activation at 140 °C.

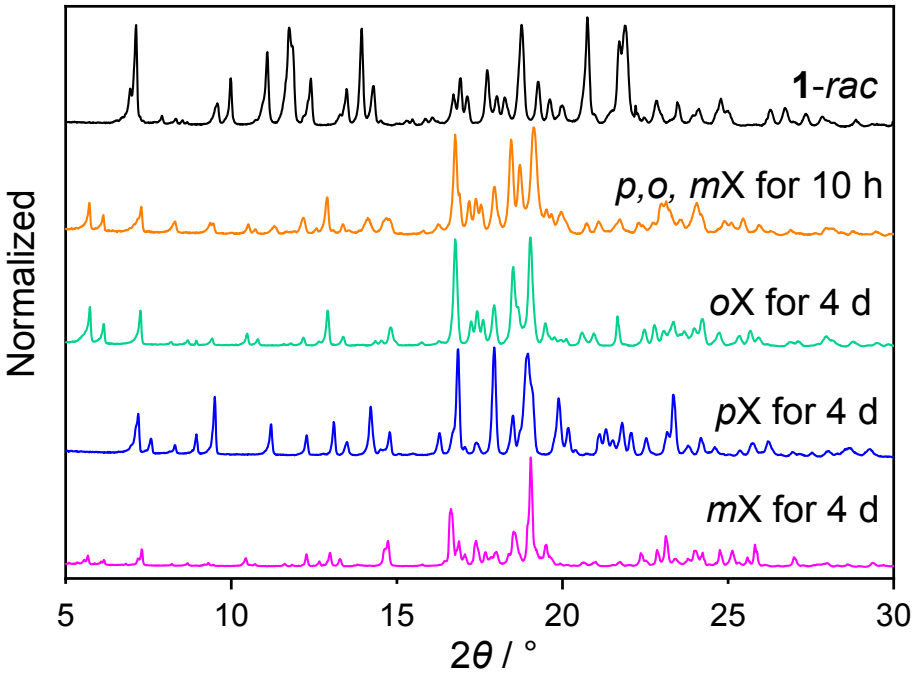

Figure S10. PXRD patterns of **1**-*rac* after exposure to xylene vapours. From bottom to top: **1**-*rac* after exposure to *m*X vapour for 4 d; **1**-*rac* after exposure to *p*X vapour for 4 d; **1**-*rac* after exposure to *o*X vapour for 4 d; **1**-*rac* after exposure to 1:1:1 pX:oX:*m*X mixture for 10 h; **1**-*rac* activated at 80 °C.

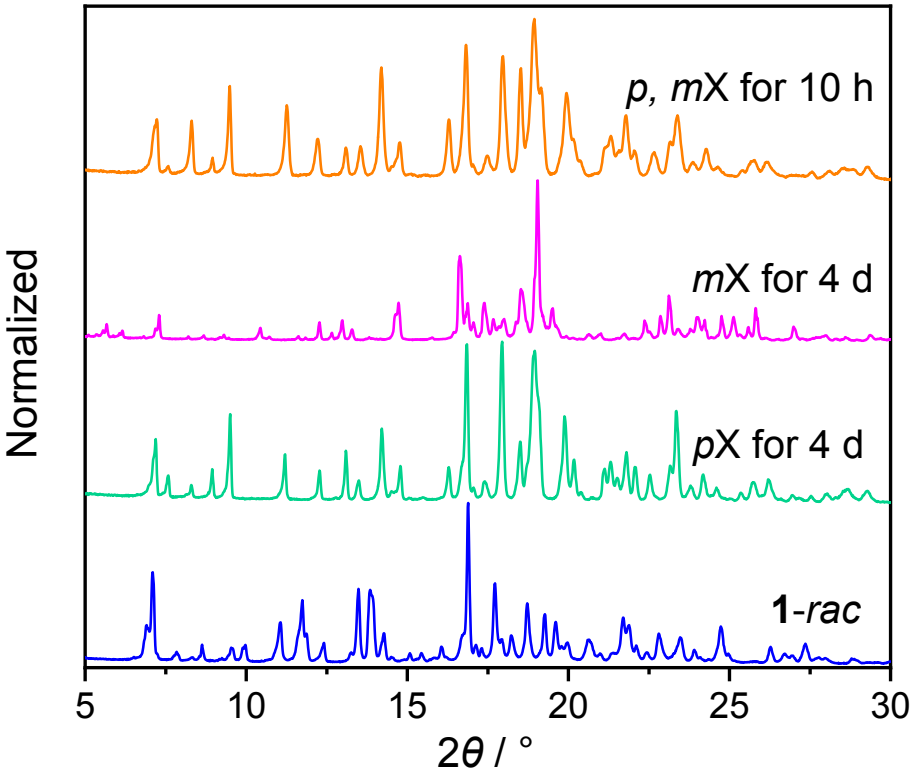

Figure S11. PXRD patterns of **1**-*rac* after exposure to xylene vapours. From bottom to top: activated **1**-*rac*; after after exposure to *p*X vapour; after exposure to *m*X vapour; after exposure to *p*X/*m*X (1:1, *vol*/*vol*) vapour mixture.

3.4 Supporting crystal structure figures

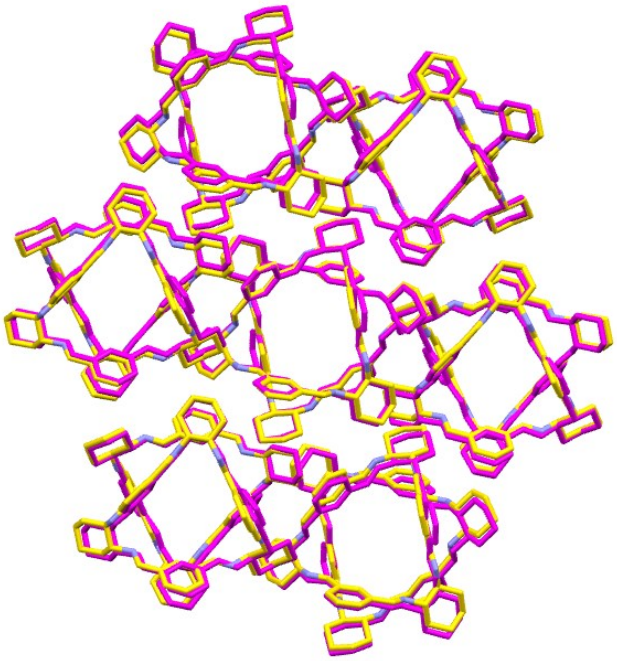

Figure S12. Crystal packing overlay for EA@**1**-*rac* (magenta) and activated **1**-*rac* (yellow), which was generated using the crystal packing similarity tool in Mercury.

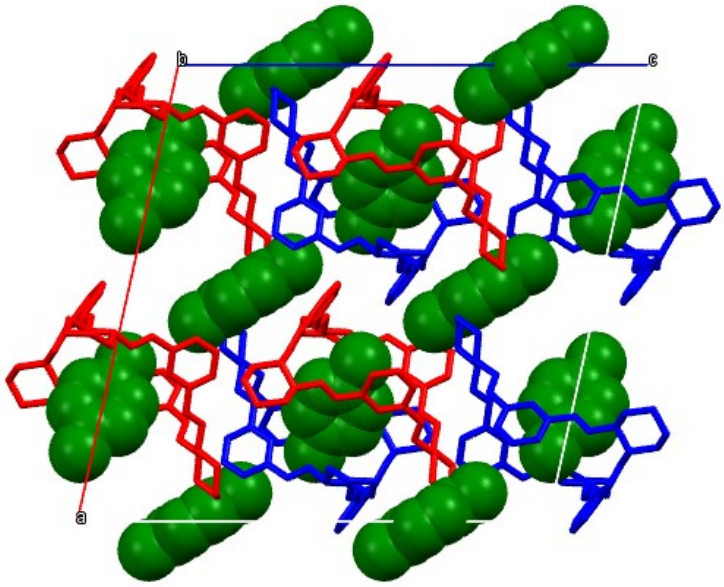

Figure S13. Crystal structure of 1 *p*X@**1**-*rac* viewed along the crystallographic *b*-axis. **1**-*R* and **1**-*S* are coloured in red and blue, respectively. H atoms are omitted for clarity.

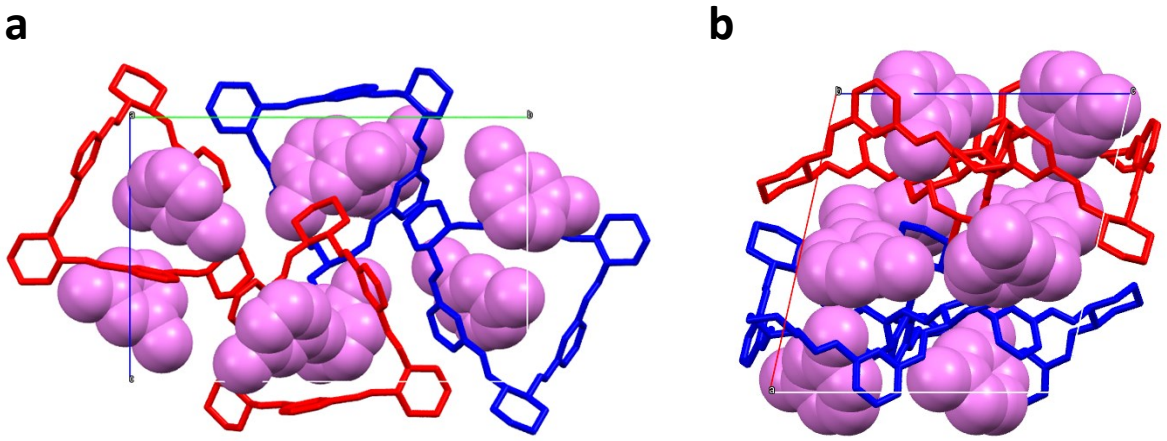

Figure S14. Crystal structure of 3*m*X@2(**1**-*rac*) viewed along the crystallographic (a) *a*-axis and (b) *b*-axis. **1**-*R* and **1**-*S* are coloured in red and blue, respectively. H atoms are omitted for clarity.

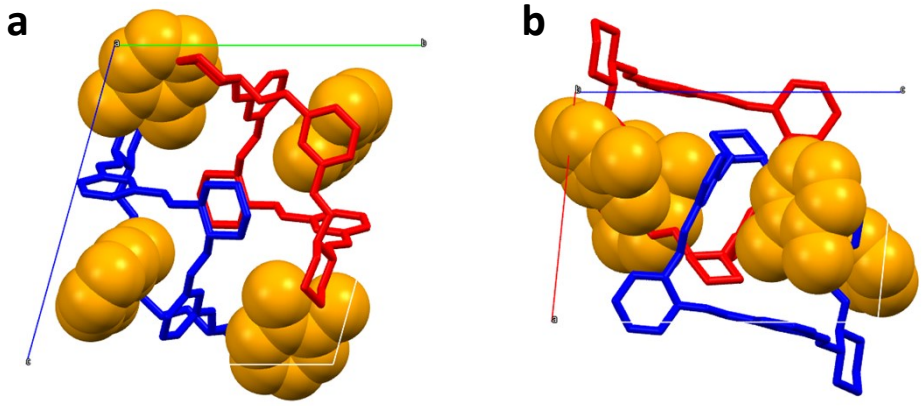

Figure S15. Crystal structure of 2*o*X@**1**-*rac* viewed along the crystallographic (a) *a*-axis and (b) *b*-axis. **1**-*R* and **1**-*S* are coloured in red and blue, respectively. H atoms are omitted for clarity.

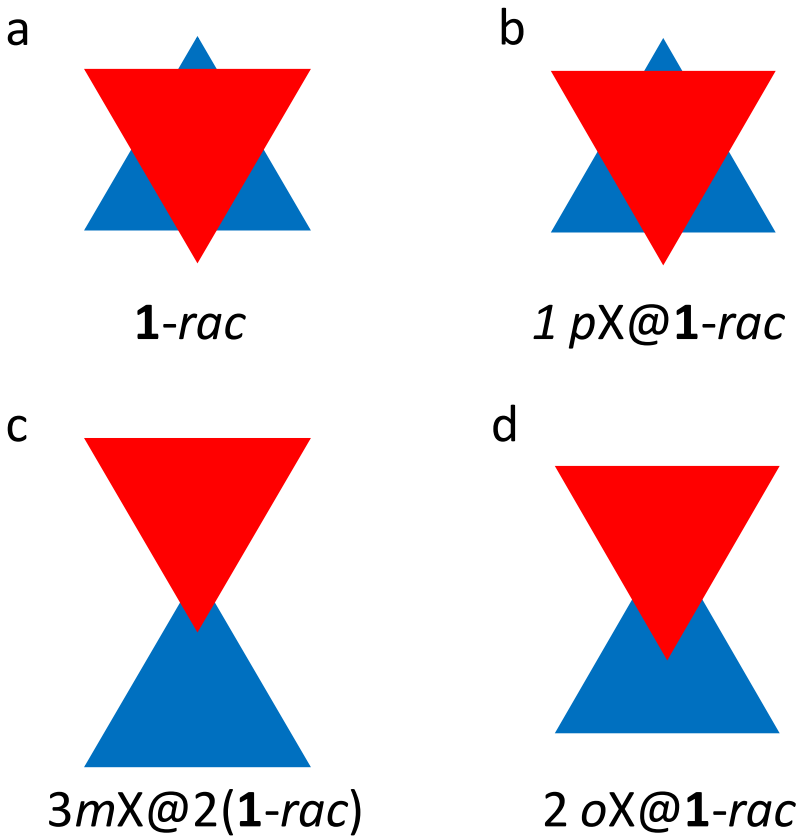

Figure S16. Schematic representation of the packing modes of the racemic **1** dimer in **1**-*rac* crystal structures. (a) **1**-*rac*, (b) 1*p*X@**1**-*rac*, (c) 3*m*X@2(**1**-*rac*), (d) 2*o*X@**1**-*rac*. **1**-*R* and **1**-*S* are coloured in red and blue, respectively.

3.5. Gas sorption

The N_2 and H_2 gas adsorption isotherms for **1**-*R* shown in Figure 1d-1e were measured using a sample that was obtained by dissolving **1**-*R* in MeOH and removing the solvent by rotary evaporator at room temperature, and then activated under vacuum at 80 °C for 12 h.

The N_2, H_2 , and CO_2 gas adsorption isotherms for **1**-*R* shown in Figure S18 were measured using a sample that was recrystallised from EA and activated under vacuum at 80 °C for 12 h.

The N_2, H_2, and CO_2 gas adsorption isotherms for **1**-*rac* were measured using a sample that was recrystallised from EA and activated under vacuum at 80 °C for 12 h.

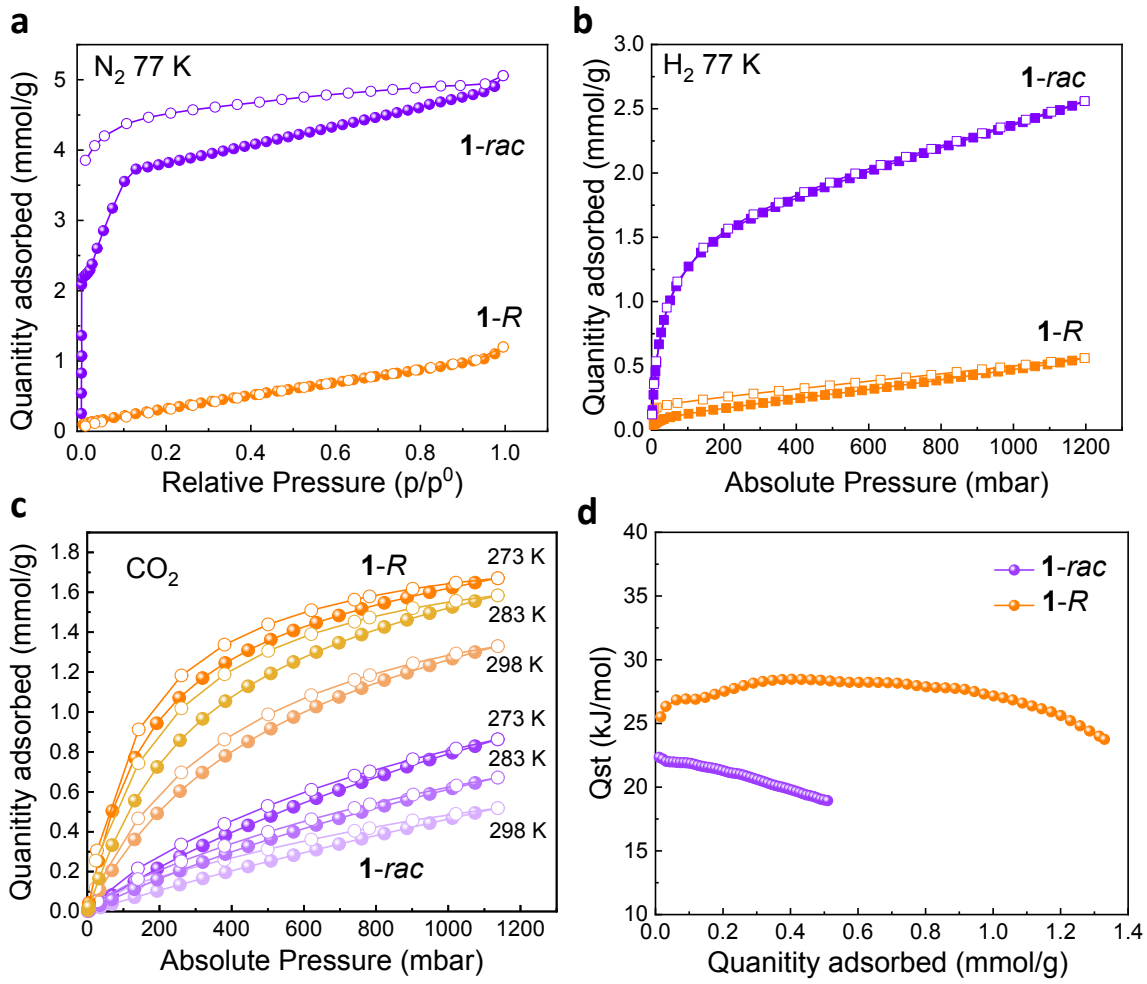

Figure S17. Gas sorption isotherms for **1**-*R* (orange) and **1**-*rac* (violet) samples that were activated from EA. (a) N_2 isotherms (77 K), (b) H_2 (77 K). (c) CO_2 isotherms at temperatures recorded between 273–298 K. Adsorption isotherms are shown using closed symbols, and desorption isotherms are shown using open symbols. (d) Isosteric heat of adsorption (Q_{st}) of CO_2 (273-298 K) for **1**-*R* and **1**-*rac*.

3.6. Isosteric heat of adsorption

The isosteric heat (*Qst*) for CO_2 adsorption with **1**-*rac and* **1**-*R* were calculated using their CO_2 isotherms measured at 273, 283, and 298 K and the Clausius-Clapyron equation:

$$\ln(P)/m = Qst/R*1/T$$

where *P* is the pressure described in bar, *m* (mmol/g) is constant quantity adsorbed, *Qst* (kJ/mol) is the isosteric heat, R [J/(mol·K)] is the gas the constant and *T* (K) is the adsorption temperature. A plot of the ln(*P*) versus 1/*T* at constant quantity adsorbed can provide a linear relationship. The slope of that line is *Qst* /R, then the *Qst* can be calculated.[6]

3.7 Selective uptake from a xylene isomers vapour mixture in 1-*rac* based on NMR

For each mixture vapour-phase experiment, an open 5 mL vial containing 3.5 mg of **1**-*rac* that was activated at 80 °C was placed in a sealed 20 mL vial containing 1 mL of *p*X:*m*X (1:1 *vol*:*vol*) or *p*X:*m*X:*o*X (1:1:1 *vol*:*vol*:*vol*). The relative uptake of guests adsorbed by the **1**-*rac* crystals was measured by completely dissolving the crystals in CD_2Cl_2 and measuring the ratio of xylene isomers to **1**-*rac* by ^1H NMR spectroscopy.

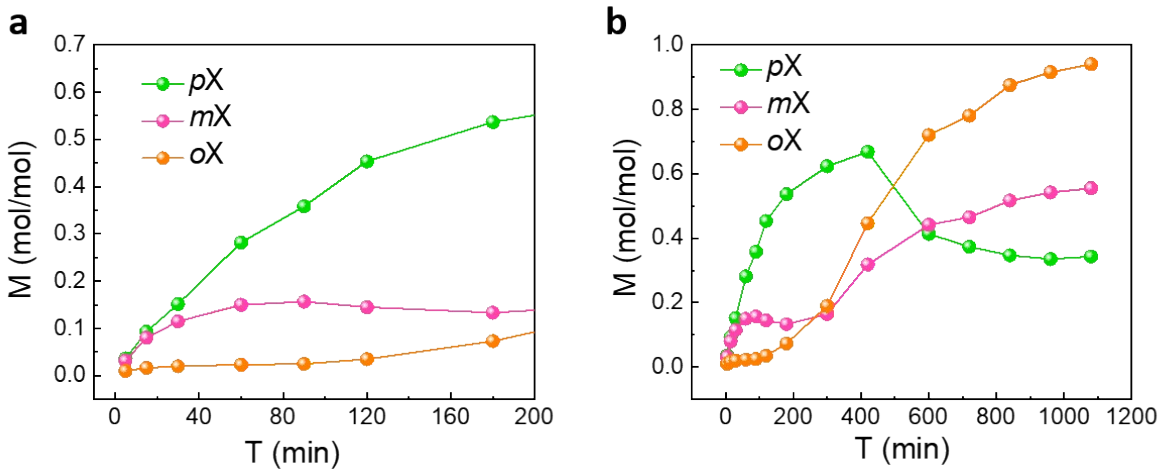

Figure S18. Time-dependent **1**-*rac* solid–vapour sorption plot for *p*X, *m*X, and *o*X from an equimolar vapour mixture, (a) over 3 hours, (b) over 18 hours.

For each adsorption–desorption cycle, an open 5 mL vial containing **1**-*rac* from the last cycle was re-activated at 140 °C under a dynamic vacuum and then placed in a sealed 20 mL vial containing 2 mL of *p*X:*m*X (1:1 *vol*:*vol*). The relative uptake of guests adsorbed by the **1**-*rac* crystals was measured by completely dissolving the crystals in CD_2Cl_2 and measuring the ratio of xylene isomers to **1**-*rac* by ^{1}H NMR spectroscopy.

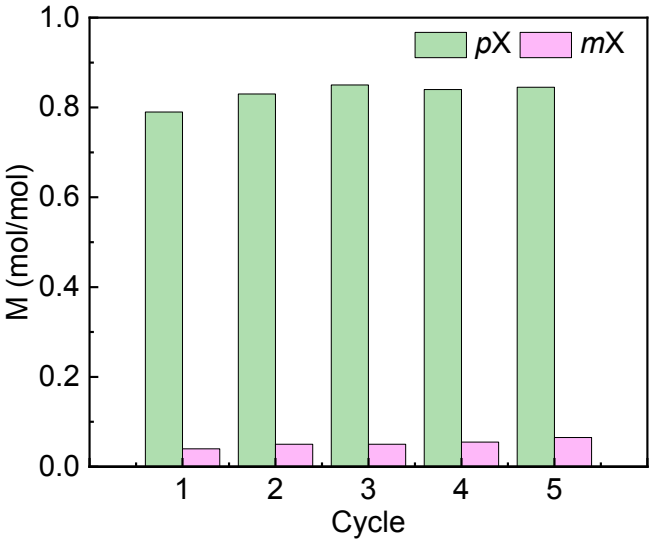

Figure S19. Adsorption–desorption cycles measured on a single sample of **1**-rac using a 1:1 *p*X:*m*X vapour mixture at room temperature. *p*X and *m*X uptakes in solid **1**-*rac* after 12 hours were calculated by ^{1}H NMR spectroscopy. Between the adsorption cycles, the material was thermally activated at 140 °C under a dynamic vacuum.

3.8. Calculation of selectivity coefficient ($K_{A:B}$)

According to equation 1, the selectivity of a host (H) for one guest (A) from a guest mixture can be described by the selectivity coefficient ($K_{A:B}$),[7] where X_A and X_B represent the molar fractions of the two competing guests in the original solution mixture, and Y_A and Y_B represent the corresponding molar fractions of the same guests in the resulting inclusion complex.[7]

$$K_{A:B} = (K_{B:A})^{-1} = Y_A/Y_B \cdot X_B/X_A \; (X_B + X_A = 1) \qquad (1)$$

References

1. G. Winter, D. G. Waterman, J. M. Parkhurst, A. S. Brewster, R. J. Gildea, M. Gerstel, L. Fuentes-Montero, M. Vollmar, T. Michels-Clark, I. D. Young, N. K. Sauter and G. Evans, *Acta Crystallogr D Struct Biol*, 2018, **74**, 85-97.
2. G. M. Sheldrick, *Acta Crystallogr. A*, 2015, **71**, 3-8.
3. G. M. Sheldrick, *Acta Crystallogr C Struct Chem*, 2015, **71**, 3-8.
4. O. V. Dolomanov, L. J. Bourhis, R. J. Gildea, J. A. K. Howard and H. Puschmann, *J. Appl. Crystallogr.*, 2009, **42**, 339-341.
5. J. Gawroński, H. Kołbon, M. Kwit and A. Katrusiak, *J. Org. Chem.*, 2000, **65**, 5768-5773.
6. S. J. Gregg, *The adsorption of gases by solids*, Methuen & co. ltd., 1934.
7. A. M. Pivovar, K. T. Holman and M. D. Ward, *Chem. Mater.*, 2001, **13**, 3018-3031.